Continuous Optical-to-Mechanical Quantum State Transfer in the Unresolved Sideband Regime

Amy Navarathna[1,2] James S. Bennett[1,2,3] and Warwick P. Bowen[1,2,*]

[1]*ARC Centre of Excellence for Engineered Quantum Systems, St Lucia, Queensland 4072, Australia*
[2]*School of Mathematics and Physics, University of Queensland, St Lucia, Queensland 4072, Australia*
[3]*Centre for Quantum Dynamics, Griffith University, Nathan, Queensland 4222, Australia*

Optical-to-mechanical quantum state transfer is an important capability for future quantum networks, quantum communication, and distributed quantum sensing. However, existing continuous state transfer protocols operate in the resolved sideband regime, necessitating a high-quality optical cavity and a high mechanical resonance frequency. Here, we propose a continuous protocol that operates in the unresolved sideband regime. The protocol is based on feedback cooling, can be implemented with current technology, and is able to transfer non-Gaussian quantum states with high fidelity. Our protocol significantly expands the kinds of optomechanical devices for which continuous optical-to-mechanical state transfer is possible, paving the way toward quantum technological applications and the preparation of macroscopic superpositions to test the fundamentals of quantum science.

The ability to transfer quantum states between optical communication channels and quantum computing nodes is a necessary ingredient of the emerging quantum internet [1]. Quantum state transfer also has important applications in quantum-enhanced sensing [2,3], quantum-secure communications [4], and fundamental tests of macroscopic quantum mechanics [5–10]. A leading approach is to mediate the transfer using an optomechanical resonator [11–16]. This is attractive because mechanical resonators interact via radiation pressure with electromagnetic fields of all frequencies [17] and can also be functionalized to interact with most quantum computing nodes, such as spins [18–20], superconducting devices [21–23], and atomic ensembles [24].

The first step in the transfer process is an optical-to-mechanical state transfer, with a subsequent transfer to the final computing node [25–27]. An optical cavity is employed to enhance the radiation pressure during the optical-to-mechanical state transfer. Leading proposals work only in the "resolved sideband regime," where the decay rate of this cavity is lower than the mechanical resonance frequency [12,28]. By contrast, most optomechanical systems operate in the "unresolved sideband regime" [29]. In many cases this is due to the benefits that low mechanical frequencies convey for applications—for instance, in precision sensing [30–32]. In others, it is because of the difficulty of simultaneously achieving a low decay rate, a high resonance frequency, and sufficient radiation pressure coupling [33].

To date, the only proposals for optical-to-mechanical state transfer in the unresolved sideband regime have used pulsed, rather than continuous, optomechanical

interactions [34–36]. This narrows the range of applications, introduces significant technical challenges due to the additional timing and phase accuracy required [36–38], and involves large radiation pressure impulse forces that can be problematic [35,39,40].

It is well known that a mechanical resonator can be feedback cooled close to its motional ground state in the unresolved sideband regime [41]. Here, we propose a continuous optical-to-mechanical state transfer protocol based on the same concept. By modeling the open quantum system dynamics, we show that feedback cooling can be understood as the transfer of a vacuum state of light onto the mechanical resonator. We find that appropriate choice of the feedback parameters allows the transfer of arbitrary quantum states. The requirements for successful transfer closely match those for ground-state cooling—once the optomechanical cooperativity exceeds the thermal occupancy of the mechanical resonator, a coherent state can be transferred with near unity fidelity and the Wigner negativity of non-Gaussian states can be preserved. Moreover, the feedback parameters can be used to phase-sensitively amplify (or "squeeze") the transferred state, to engineer its temporal profile, and—in direct analogy to state-transfer via resolved sideband cooling [42]—to achieve the transfer of a single optical sideband.

Our work extends continuous optomechanical state transfer beyond the resolved sideband limit to low-quality optical cavities and low frequency mechanical resonators. Feedback cooling of a mechanical resonator to near its motional ground state has recently been demonstrated, both in cryogenic [43] and room temperature environments [44]. As such, our proposal can be directly implemented with
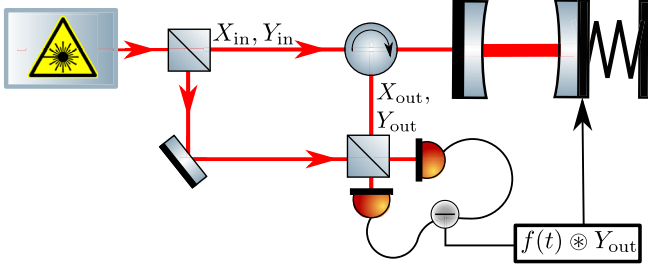
FIG. 1. Schematic optomechanical system with feedback. Light is coupled into an optomechanical cavity. The reflected light is measured through homodyne detection. The detected photocurrent $[Y_{\text{out}}(t)]$ is convolved with a filter $f(t)$ and directly fed back to the momentum of the mechanical resonator.

existing technology, providing a new tool for quantum networks and opening a new pathway to create and study macroscopic quantum systems. Our work also provides new insights into feedback cooling, showing that the process is in fact a quantum state transfer from light to mechanical motion. These insights may also be applicable in the resolved sideband regime, where feedback-induced "squashing" has been shown to improve cooling [45].

We consider an optomechanical system in the unresolved sideband, high mechanical quality regime ($\kappa \gg \Omega \gg \Gamma$) with resonant optical driving, where κ (Γ) is the optical (mechanical) energy decay rate, and Ω the mechanical resonance frequency. In this scenario, the amplitude quadrature of the input optical field X_{in} is directly imprinted on the mechanical motion via radiation pressure. The phase quadrature Y_{in} is not, but is encoded on the phase quadrature of the output optical field as [17]

$$Y_{\text{out}} = -\sqrt{\eta}Y_{\text{in}} + 2\sqrt{\eta\Gamma C}Q + \sqrt{1-\eta}Y_{\text{v}}, \qquad (1)$$

where η is the detection efficiency, $C = 4g_{\text{om}}^2/\Gamma\kappa$ is the optomechanical cooperativity with g_{om} being the coherent-amplitude-boosted optomechanical coupling rate, Y_{v} is the vacuum noise introduced due to detection loss, Q (P) is the dimensionless mechanical position (momentum) operator with $[Q, P] = i$, and all optical quadrature operators are normalized such that $[X(t), Y(t')] = i\delta(t - t')$. We propose to detect the output phase quadrature and use continuous feedback to transfer it to the mechanical resonator, as shown in Fig. 1. We note that feed-forward, similar to our feedback, has been applied to improve microwave-to-optical state transfer in the resolved sideband regime [46]. In contrast, the feed-forward in that experiment functioned to suppress correlated noise terms, while both optical quadratures were transferred by radiation pressure. A transduction scheme between two different-frequency fields has also been proposed in the unresolved sideband regime [47]. That work does not explore optical-to-mechanical state transfer and, unlike our proposal, assumes a dissipationless mechanical resonator ($\Gamma = 0$).

Our scheme is analogous to feedback cooling [41,43,44,48–52], with the detected signal applied as a force onto the mechanical resonator. This force could be applied, for instance, using radiation pressure [45] or electrostatic actuation [51]. In either case, a quantum transfer requires that the electronic noise floor of the detector is well beneath the quantum noise of the light, a criterion that has been achieved in many experiments (e.g., [45]). Using quantum Langevin equations, we find that it is described by the following equations of motion:

$$\dot{Q} = \Omega P - \frac{\Gamma}{2}Q + \sqrt{\Gamma}Q_{\text{in}}, \qquad (2)$$

and

$$\dot{P} = -\Omega Q - \frac{\Gamma}{2}P + \sqrt{\Gamma}P_{\text{in}} - 2\sqrt{\Gamma C}X_{\text{in}} - \frac{\Gamma G}{2}f(t)$$

$$\circledast \left(-\left(Y_{\text{in}} - \sqrt{\frac{1-\eta}{\eta}}Y_{\text{v}} \right)\frac{1}{2\sqrt{\Gamma C}} + Q \right), \qquad (3)$$

where P_{in} and Q_{in} are white thermal noise operators that satisfy $[Q_{\text{in}}(t), P_{\text{in}}(t')] = i\delta(t - t')$, and we have made the rotating wave approximation with respect to the mechanical bath [17,53]. The last term of Eq. (3) represents the feedback force, where the measured photocurrent is convolved with an arbitrary causal filter function $f(t) \in \mathbb{R}$ and amplified by the gain factor G. The filter function is normalized so that $|f(\Omega)| = 1$, where $f(\omega) = \int_{-\infty}^{\infty} f(t)e^{i\omega t}dt$ is the Fourier transform of $f(t)$.

The steady-state solutions to Eqs. (2) and (3) are found by moving into frequency space and adiabatically eliminating the dynamics of the optical cavity field (Supplemental Material, Sec. I [54]). This results in the quadratures

$$Q(\omega) = \sqrt{\Gamma}\chi(\omega)\left[Q_{\text{in}} + \phi(\omega)P_{\text{in}} - 2\sqrt{C}\phi(\omega)X_{\text{in}} \right.$$

$$\left. + \frac{Gf(\omega)\phi(\omega)}{4\sqrt{C}}\left(Y_{\text{in}} - \sqrt{\frac{1-\eta}{\eta}}Y_{\text{v}} \right) \right], \qquad (4)$$

$$P(\omega) = \sqrt{\Gamma}\chi(\omega)\left[P_{\text{in}} - \left(\frac{Gf(\omega)\Gamma}{2\Omega} + 1 \right)\phi(\omega)Q_{\text{in}} \right.$$

$$\left. - 2\sqrt{C}X_{\text{in}} + \frac{Gf(\omega)}{4\sqrt{C}}\left(Y_{\text{in}} - \sqrt{\frac{1-\eta}{\eta}}Y_{\text{v}} \right) \right], \qquad (5)$$

where

$$\phi(\omega) = \frac{\Omega}{\Gamma/2 - i\omega}, \qquad (6)$$

the feedback-broadened mechanical susceptibility is

$$\chi(\omega) = \frac{1}{\Omega\phi(\omega)^{-1} + [\Omega + G\Gamma\frac{f(\omega)}{2}]\phi(\omega)}, \qquad (7)$$

and the adiabatic elimination is valid in the unresolved sideband regime ($\{\Omega, C\Gamma\} \ll \kappa$) taken throughout this Letter. From Eq. (7), we see that the mechanical susceptibility decreases as G increases. This suppresses most of the mechanical terms in Eqs. (4) and (5). The only term that remains is Q_{in} in $P(\omega)$, but this is suppressed by the large mechanical quality factor ($\Omega/\Gamma \gg 1$). It is this combined suppression of all mechanical terms that enables optical state transfer with high fidelity.

The optical input field consists of a continuum of optical modes. To build insight into which of these modes is best transferred to the single mechanical mode, as well as to identify the gain and noise of the transfer process, we rewrite Eqs. (4) and (5) as

$$Q = g_X X_{\text{trans}} + Q_{\text{noise,optical}} + Q_{\text{noise,mechanical}}, \quad (8)$$

$$P = g_Y Y_{\text{trans}} + P_{\text{noise,optical}} + P_{\text{noise,mechanical}}. \quad (9)$$

Here, X_{trans} and Y_{trans} define the optical quadratures transferred to position and momentum, respectively, in each case including contributions from both X_{in} and Y_{in} [see Eqs. (10) and (11)]. g_X and g_Y are the transfer gains. Terms labeled with a subscript "noise" encompass the residual thermal variance remaining after feedback, and any optical terms not arising from the temporal mode of interest (i.e., inefficient detection, mode mismatch). In what follows, we will quantify each term in these equations.

The input optical quadratures transferred to Q and P in Eqs. (4) and (5) are not perfectly conjugate observables. The difference is embodied in $\phi(\omega)$, and is a result of the retarded response of the mechanical position to an applied force. The imperfection introduces an ambiguity in the optical mode that is optimally transferred—a different mode is best transferred to P and Q. Here, we choose to assess the transfer of the mode that is optimally transferred to P. Justifying the choice, we find that this mode can be transferred with fidelity approaching unity for high mechanical quality factors [e.g., see Fig. 3(b)].

Optimal transfer to P implies that the optical input terms in Eq. (5) will make no contribution to the optical noise term in Eq. (9), that is, they will be entirely contained within the $g_Y Y_{\text{trans}}$ term. By comparing Eqs. (5) and (9), Y_{trans} can then be immediately identified as

$$Y_{\text{trans}} = \frac{2\sqrt{\Gamma C}}{g_Y} \chi(\omega) \left(-X_{\text{in}} + \frac{G f(\omega)}{8C} Y_{\text{in}} \right). \quad (10)$$

X_{trans} can be determined by rotating Y_{trans} by $\pi/2$ in phase space ($Y \to X$ and $X \to -Y$ for all X and Y quadratures). This gives

$$X_{\text{trans}} = \frac{2\sqrt{\Gamma C}}{g_Y} \chi(\omega) \left(\frac{G f(\omega)}{8C} X_{\text{in}} + Y_{\text{in}} \right). \quad (11)$$

Using the relation $a_{\text{trans}} = (X_{\text{trans}} + iY_{\text{trans}})/\sqrt{2}$ then yields the annihilation operator of the transferred mode

$$a_{\text{trans}}(\omega) = u(\omega) a_{\text{in}}(\omega), \quad (12)$$

where

$$u(\omega) = \frac{2\sqrt{\Gamma C}}{g_Y} \chi(\omega) \left(\frac{G f(\omega)}{8C} - i \right) \quad (13)$$

is its spectral mode shape and $a_{\text{in}}(\omega) = [X_{\text{in}}(\omega) + iY_{\text{in}}(\omega)]/\sqrt{2}$.

The phase quadrature transfer gain, g_Y, can be determined by enforcing the boson commutation relation $[a_{\text{trans}}(t), a_{\text{trans}}^\dagger(t)] = 1$ on Eq. (12). Recognizing that the optical noise must originate from an orthogonal optical mode to the transferred mode, the amplitude quadrature gain, g_X, can be found by enforcing the commutation relations $[Q_{\text{noise,optical}}(t), X_{\text{trans}}(t)] = [Q_{\text{noise,optical}}(t), Y_{\text{trans}}(t)] = 0$, where $Q_{\text{noise,optical}}$ is obtained by rearranging Eq. (8). Together, these give

$$g_Y = \left[\frac{4\Gamma C}{2\pi} \int_{-\infty}^{\infty} |\chi(\omega)|^2 (|f(\omega)|^2 + 1) d\omega \right]^{1/2}, \quad (14)$$

$$g_X = -\frac{1}{g_Y} \frac{8\Gamma C}{2\pi} \int_{-\infty}^{\infty} |\chi(\omega)|^2 \Im[\phi(\omega)] \Im[f(\omega)] d\omega. \quad (15)$$

The spectral mode shape and quadratures of the transferred mode depend on both the feedback-broadened mechanical susceptibility $\chi(\omega)$ and the feedback filter function $f(\omega)$, so that the transferred state can be controlled through appropriate choice of the filter properties. Thus far, our results are valid for an arbitrary real-valued causal filter function. In the remainder of the Letter we choose the generalized-Lorentzian filter

$$f(\omega) = \frac{\Gamma' \Omega}{\omega^2 - \Omega^2 + i\Gamma' \omega}, \quad (16)$$

where Γ' is the filter bandwidth. This filter is commonly used for feedback cooling [41,50,52,55] and is close to the known optimal filter for both momentum estimation [56] and feedback cooling [57]. Γ' is chosen to be much larger than Ω, so that the filter acts as an integrator near the mechanical resonance frequency. The gain factor G can then be understood as the fractional increase in the mechanical decay rate due to the feedback.

With the filter in Eq. (16) and in the limit of large filter bandwidth and mechanical quality factor ($\Omega/\Gamma \gg 1$), the amplitude and phase quadrature transfer gains can be approximated as

$$g_Y = 2\sqrt{C \left(\frac{1 + \frac{G^2}{64C^2}}{2 + G} \right)} \quad \text{and} \quad g_X = \frac{1}{g_Y(1 + 2/G)}. \quad (17)$$
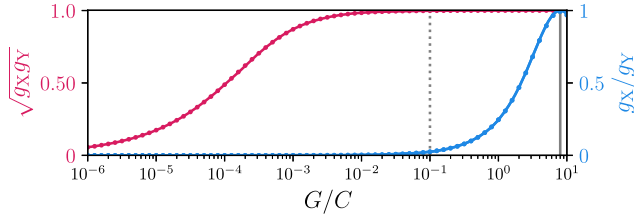
FIG. 2. Transfer gain ($\sqrt{g_X g_Y}$, red) and squeezing (g_X/g_Y, blue) as a function of the feedback strength by cooperativity (G/C). The dashed line indicates G = 1 and the full gray line indicates the optimal gain (G = 8C), where $g_X/g_Y = 1$. The dots are numerically obtained, and the lines are using the analytic expressions derived in the high-quality factor limit.

We define the overall gain of the transfer process as $\sqrt{g_X g_Y}$, so that it is independent of unitary squeezing operations on the transferred state [58], and define the level of squeezing applied during the transfer as g_X/g_Y. The overall gain and squeezing level are plotted as a function of the feedback gain factor G in Fig. 2 using both numerical calculations and the analytic approximations of Eqs. (17). For these plots and throughout the Letter we use the system parameters $\Omega/2\pi = 1$ MHz, $\Gamma/2\pi = 1$ Hz, $\Gamma'/2\pi = 1.59$ MHz, $\kappa/2\pi = 100$ MHz, $g_{om}/2\pi = 395$ kHz, and $T = 30$ mK, corresponding to a thermal phonon occupancy $n_{th} \sim k_B T/\hbar\Omega \sim 620$. These parameters have been achieved in a range of optomechanical experiments [33,43,44].

The overall transfer gain asymptotes unity in the experimentally relevant limit where $G \gg 1$. This means that the state transfer is intrinsically robust to variations in G. The transfer generally involves amplitude quadrature squeezing ($g_X/g_Y < 1$). Only at G = 8C do we find that the input state is transferred without any squeezing ($g_X/g_Y = 1$). Comparison of Eq. (11) with Eq. (4) shows that, in the high-quality limit for which $f(\omega)$ can be substituted with $f(\pm\Omega) = \mp i$ and $\phi(\omega)$ with $\phi(\pm\Omega) = \pm i$, this choice of gain also results in near agreement between X_{trans} and the optical input terms in Q. The remaining discrepancy arises from the retardation factor $\phi(\omega)$, and this discrepancy approaches zero in the high-quality factor limit. We therefore select G = 8C for the remainder of the Letter.

It is illustrative to consider how our choice of filter function and gain factor influences the spectral mode shape $u(\omega)$. The frequency dependence of the prefactor in Eq. (13) depends only on $\chi(\omega)$, and is sharply peaked at both $\pm\Omega$. However, since $f(\pm\Omega) = \mp i$, for G = 8C the term in parentheses is precisely zero at $-\Omega$ and equals $-2i$ at Ω. Our particular choice, therefore, enables a single-sideband state transfer, transferring only the lower optical sideband and doing this with a mode shape given approximately by $\chi(\omega)$ (see also Supplemental Material, Sec. II [54]).

To quantitatively assess the quality of transfer we first consider an input vacuum state. We calculate the contributions to the position and momentum variances from this input and from the noise sources specified in Eqs. (8)
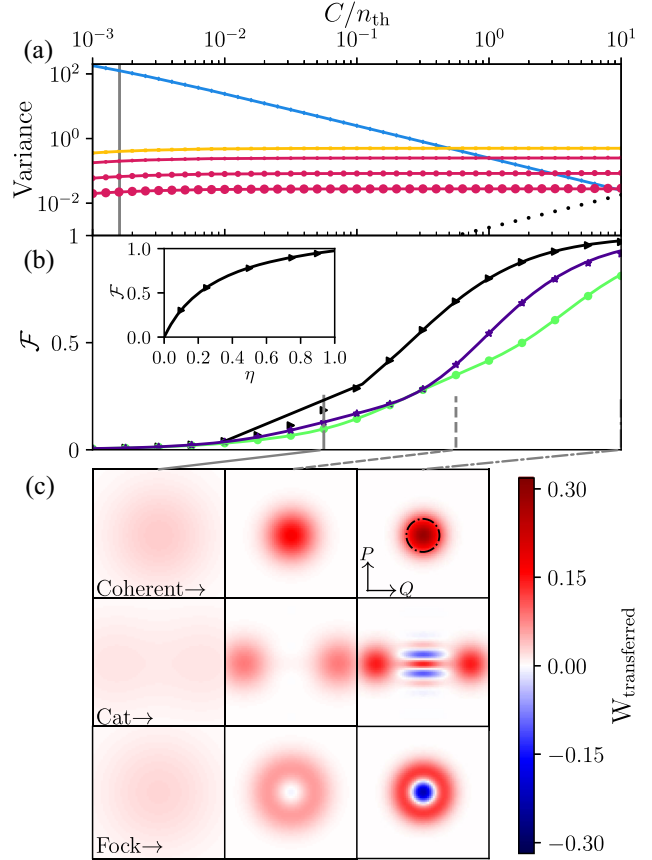

FIG. 3. (a) Contributions to the variance as a function of interaction strength of mechanical noise (blue), optical signal (yellow), and two contributions of optical noise: mode mismatch on Q (black), and inefficiency (red). The size of the points correspond to the inefficiency ($\eta = 0.9, 0.75$, and 0.5 for small, medium, and large points, respectively). (b) The transfer fidelity ($\mathcal{F}$) as a function of interaction strength for a coherent state (black), cat state (green) ($\alpha = 2$), and single photon Fock state (dark blue). Inset shows $\mathcal{F}$ as a function of η for the coherent state, at a fixed value of $C/n_{th} = 10$ corresponding, for our parameters, to an optomechanical cooperativity of $C \sim 6200$. (c) Corresponding plots of the Wigner distributions for a coherent state (top row), cat state (middle row), and Fock state (bottom row) at the interaction strengths indicated by the gray lines connected to subplot (b). The black dotted circle in the top right indicates the length scale of the contour of the ground state. The orientation of the plots is indicated by the black arrows in the top right plot.

and (9) (see Supplemental Material, Secs. II and III [54]). We separate the optical noise into contributions arising from inefficiencies and mode mismatch, so that the nonideality of the transfer that arises due to $\phi(\omega)$ can be assessed. The results are plotted in Fig. 3(a) as a function of C/n_{th} (with G = 8C). The variance of the transferred optical mode increases with C, asymptoting to the vacuum variance of 1/2 once $C \gg 1$. Conversely, the mechanical noise contribution decreases, dropping below the vacuum level for $C \gg n_{th}$. The variance of the optical inefficiency

noise has a cooperativity dependence that is similar to the optical signal, increasing with C and asymptoting to a constant value once $C \gg 1$. As expected, this noise increases as the detection efficiency degrades. However, even for η as low as 0.5 the transferred signal variance still dominates inefficiency noise for the whole range of C/n_{th}. The mode-mismatch noise on Q is very low for small C, increases approximately linearly with C, and eventually exceeds the signal variance. Thus, the mode mismatch ultimately constrains the performance of the state transfer. In future work it would be interesting to consider different choices of transferred mode to potentially relax this constraint.

Using the analytic expressions for the gains in Eqs. (17), we derive analytic expressions for the different variance contributions that are valid in the same high-quality, high-bandwidth limit (see Supplemental Material [54], Sec. III). With the exception of the mismatch noise, which is zero in the limit of high quality, these expressions agree well with the numerical results in Fig. 3(a). From them, we find that when $C \gg 1$ the noise variance introduced by optical inefficiency is $V_\eta = (1 - \eta)/4\eta$, and that the mechanical noise variance is suppressed below the vacuum noise level once $C > n_{\text{th}}/2$.

Since the feedback process is linear and all noise sources are Gaussian, it is straightforward to extend our analysis beyond the transfer of vacuum states to more elaborate states such as Schrödinger cat states. This can be achieved using Wigner functions (Supplemental Material, Sec. IV [54]). Imperfections introduced by the thermal noise, mode mismatch, and inefficiency tend to "smear out" quantum features of the transferred optical mode's Wigner function. Mathematically, this is represented by convolving the signal's Wigner function with a Gaussian noise kernel $\mathcal{G}(\boldsymbol{r})$ [with $\boldsymbol{r} = (Q\,P)^T$] [59]:

$$W_{\text{transferred}}(\boldsymbol{r}) = (W \circledast \mathcal{G})(\boldsymbol{r}). \tag{18}$$

In the regime relevant to this Letter, $\mathcal{G}$ is typically close to symmetric, with a slight wider spread in the Q direction due to mode mismatch. The transfer fidelity can then be determined for any pure input state as

$$\mathcal{F} = 2\pi \int_{-\infty}^{\infty} \int_{-\infty}^{\infty} W(\boldsymbol{r}) W_{\text{transferred}}(\boldsymbol{r}) d^2\boldsymbol{r}. \tag{19}$$

We plot the fidelity for input coherent, Fock, and cat states in Fig. 3(b) as a function of C/n_{th} and assuming that $\eta = 1$. The coherent state fidelity exceeds the classical limit of $1/2$ at $C/n_{\text{th}} = 0.25$ and the no-cloning bound of $2/3$ at $C/n_{\text{th}} = 0.50$. The fidelity for the non-Gaussian states also reach fidelities greater than 0.5 at similar, experimentally accessible [33,43,60] cooperativities. For the chosen experimental parameters, the maximum achievable fidelities are 0.98, 0.93, and 0.82 for coherent, Fock, and cat states, respectively, and are limited by the mode-mismatch noise. The fidelity is robust against measurement inefficiencies as visible in the inset of Fig. 3(b), which shows that the

coherent state fidelity can exceed $1/2$ even with a detection efficiency as low as $\eta = 0.2$. It is also robust against variations in feedback gain (see Supplemental Material, Sec. V [54]). Figure 3(c) plots the Wigner distributions of transferred coherent, Fock, and cat states at three different values of C/n_{th}, showing that the negativity of the Fock and cat states can be transferred, and therefore nonclassical properties of the input state preserved. The ability to achieve fidelities approaching unity and preserve nonclassical properties indicates that our scheme could be used effectively in a diverse range of quantum protocols, from optical-to-microwave state transfer to quantum memories.

In conclusion, we have identified that feedback can be used to achieve continuous optical-to-mechanical state transfer in the unresolved sideband regime. We predict that state transfer can be achieved with high fidelity and while preserving nonclassical features such as Wigner negativity. The ability to implement continuous state transfer in the unresolved sideband regime significantly widens the class of optomechanical systems that can be used as interfaces in quantum networks.

---

[*]Corresponding author.
w.bowen@uq.edu.au

[1] H. J. Kimble, Nature (London) **453**, 1023 (2008).

[2] C. L. Degen, F. Reinhard, and P. Cappellaro, Rev. Mod. Phys. **89**, 035002 (2017).

[3] D. Lachance-Quirion, S. P. Wolski, Y. Tabuchi, S. Kono, K. Usami, and Y. Nakamura, Science **367**, 425 (2020).

[4] R. Riedinger, A. Wallucks, I. Marinković, C. Löschnauer, M. Aspelmeyer, S. Hong, and S. Gröblacher, Nature (London) **556**, 473 (2018).

[5] M. Paternostro, D. Vitali, S. Gigan, M. S. Kim, Č. Brukner, J. Eisert, and M. Aspelmeyer, Phys. Rev. Lett. **99**, 250401 (2007).

[6] I. Pikovski, M. R. Vanner, M. Aspelmeyer, M. S. Kim, and Č. Brukner, Nat. Phys. **8**, 393 (2012).

[7] M. Arndt and K. Hornberger, Nat. Phys. **10**, 271 (2014).

[8] S. Forstner, M. Zych, S. Basiri-Esfahani, K. E. Khosla, and W. P. Bowen, Optica **7**, 1427 (2020).

[9] S. Kotler, G. A. Peterson, E. Shojaee, F. Lecocq, K. Cicak, A. Kwiatkowski, S. Geller, S. Glancy, E. Knill, R. W. Simmonds et al., Science **372**, 622 (2021).

[10] L. Mercier de Lépinay, C. F. Ockeloen-Korppi, M. J. Woolley, and M. A. Sillanpää, Science **372**, 625 (2021).

[11] S. Barzanjeh, M. Abdi, G. J. Milburn, P. Tombesi, and D. Vitali, Phys. Rev. Lett. **109**, 130503 (2012).

[12] T. A. Palomaki, J. W. Harlow, J. D. Teufel, R. W. Simmonds, and K. W. Lehnert, Nature (London) **495**, 210 (2013).

[13] R. W. Andrews, A. P. Reed, K. Cicak, J. D. Teufel, and K. W. Lehnert, Nat. Commun. **6,** 10021 (2015).

[14] N. J. Lambert, A. Rueda, F. Sedlmeir, and H. G. L. Schwefel, Adv. Quantum Technol. **3,** 1900077 (2020).

[15] G. Arnold, M. Wulf, S. Barzanjeh, E. S. Redchenko, A. Rueda, W. J. Hease, F. Hassani, and J. M. Fink, Nat. Commun. **11,** 4460 (2020).

[16] M. Mirhosseini, A. Sipahigil, M. Kalaee, and O. Painter, Nature (London) **588,** 599 (2020).

[17] W. P. Bowen and G. J. Milburn, *Quantum Optomechanics* (CRC Press, Boca Raton, London, New York, 2015), ISBN 978-0-367-57519-9.

[18] P. Rabl, P. Cappellaro, M. V. Gurudev Dutt, L. Jiang, J. R. Maze, and M. D. Lukin, Phys. Rev. B **79,** 041302(R) (2009).

[19] P. Ovartchaiyapong, K. W. Lee, B. A. Myers, and A. C. B. Jayich, Nat. Commun. **5,** 4429 (2014).

[20] S. G. Carter, A. S. Bracker, G. W. Bryant, M. Kim, C. S. Kim, M. K. Zalalutdinov, M. K. Yakes, C. Czarnocki, J. Casara, M. Scheibner *et al.*, Phys. Rev. Lett. **121,** 246801 (2018).

[21] B. H. Schneider, S. Etaki, H. S. J. van der Zant, and G. A. Steele, Sci. Rep. **2,** 599 (2012).

[22] P. Arrangoiz-Arriola, E. A. Wollack, M. Pechal, J. D. Witmer, J. T. Hill, and A. H. Safavi-Naeini, Phys. Rev. X **8,** 031007 (2018).

[23] M. Pechal, P. Arrangoiz-Arriola, and A. H. Safavi-Naeini, Quantum Sci. Technol. **4,** 015006 (2018).

[24] P. Treutlein, D. Hunger, S. Camerer, T. W. Hansch, and J. Reichel, Phys. Rev. Lett. **99,** 140403 (2007).

[25] W. Hease, A. Rueda, R. Sahu, M. Wulf, G. Arnold, H. G. L. Schwefel, and J. M. Fink, PRX Quantum **1,** 020315 (2020).

[26] P. K. Shandilya, D. P. Lake, M. J. Mitchell, D. D. Sukachev, and P. E. Barclay, Nat. Phys. **17,** 1420 (2021).

[27] B. M. Brubaker, J. M. Kindem, M. D. Urmey, S. Mittal, R. D. Delaney, P. S. Burns, M. R. Vissers, K. W. Lehnert, and C. A. Regal, Phys. Rev. X **12,** 021062 (2022).

[28] J. Zhang, K. Peng, and S. L. Braunstein, Phys. Rev. A **68,** 013808 (2003).

[29] M. Aspelmeyer, T. J. Kippenberg, and F. Marquardt, Rev. Mod. Phys. **86,** 1391 (2014).

[30] S. Basiri-Esfahani, A. Armin, S. Forstner, and W. P. Bowen, Nat. Commun. **10,** 132 (2019).

[31] M. Sansa, M. Defoort, A. Brenac, M. Hermouet, L. Banniard, A. Fafin, M. Gely, C. Masselon, I. Favero, G. Jourdan *et al.*, Nat. Commun. **11,** 3781 (2020).

[32] B. Abbott, R. Abbott, R. Adhikari, P. Ajith, B. Allen, G. Allen, R. Amin, S. B. Anderson, W. G. Anderson, M. A. Arain *et al.*, New J. Phys. **11,** 073032 (2009).

[33] R. Leijssen, G. R. La Gala, L. Freisem, J. T. Muhonen, and E. Verhagen, Nat. Commun. **8,** ncomms16024 (2017).

[34] M. R. Vanner, I. Pikovski, G. D. Cole, M. S. Kim, Č. Brukner, K. Hammerer, G. J. Milburn, and M. Aspelmeyer, Proc. Natl. Acad. Sci. U.S.A. **108,** 16182 (2011).

[35] J. S. Bennett, K. Khosla, L. S. Madsen, M. R. Vanner, H. Rubinsztein-Dunlop, and W. P. Bowen, New J. Phys. **18,** 053030 (2016).

[36] U. B. Hoff, J. Kollath-Bönig, J. S. Neergaard-Nielsen, and U. L. Andersen, Phys. Rev. Lett. **117,** 143601 (2016).

[37] M. R. Vanner, J. Hofer, G. D. Cole, and M. Aspelmeyer, Nat. Commun. **4,** 2295 (2013).

[38] K. E. Khosla, G. A. Brawley, M. R. Vanner, and W. P. Bowen, Optica **4,** 1382 (2017).

[39] J. T. Muhonen, G. R. La Gala, R. Leijssen, and E. Verhagen, Phys. Rev. Lett. **123,** 113601 (2019).

[40] J. S. Bennett, L. S. Madsen, H. Rubinsztein-Dunlop, and W. P. Bowen, New J. Phys. **22,** 103028 (2020).

[41] S. Mancini, D. Vitali, and P. Tombesi, Phys. Rev. Lett. **80,** 688 (1998).

[42] R. W. Peterson, T. P. Purdy, N. S. Kampel, R. W. Andrews, P.-L. Yu, K. W. Lehnert, and C. A. Regal, Phys. Rev. Lett. **116,** 063601 (2016).

[43] M. Rossi, D. Mason, J. Chen, Y. Tsaturyan, and A. Schliesser, Nature (London) **563,** 53 (2018).

[44] J. Guo, R. Norte, and S. Gröblacher, Phys. Rev. Lett. **123,** 223602 (2019).

[45] M. Rossi, N. Kralj, S. Zippilli, R. Natali, A. Borrielli, G. Pandraud, E. Serra, G. Di Giuseppe, and D. Vitali, Phys. Rev. Lett. **119,** 123603 (2017).

[46] A. P. Higginbotham, P. S. Burns, M. D. Urmey, R. W. Peterson, N. S. Kampel, B. M. Brubaker, G. Smith, K. W. Lehnert, and C. A. Regal, Nat. Phys. **14,** 1038 (2018).

[47] H. K. Lau and A. A. Clerk, Phys. Rev. Lett. **124,** 103602 (2020).

[48] P. F. Cohadon, A. Heidmann, and M. Pinard, Phys. Rev. Lett. **83,** 3174 (1999).

[49] A. Hopkins, K. Jacobs, S. Habib, and K. Schwab, Phys. Rev. B **68,** 235328 (2003).

[50] M. Poggio, C. L. Degen, H. J. Mamin, and D. Rugar, Phys. Rev. Lett. **99,** 017201 (2007).

[51] K. H. Lee, T. G. McRae, G. I. Harris, J. Knittel, and W. P. Bowen, Phys. Rev. Lett. **104,** 123604 (2010).

[52] G. I. Harris, U. L. Andersen, J. Knittel, and W. P. Bowen, Phys. Rev. A **85,** 061802(R) (2012).

[53] A. C. Doherty, A. Szorkovszky, G. I. Harris, and W. P. Bowen, Phil. Trans. R. Soc. A **370,** 5338 (2012).

[54] See Supplemental Material at http://link.aps.org/supplemental/10.1103/PhysRevLett.130.263603 for more details to reproduce the work, a figure of the contributions to the power spectral density of the mechanical quadratures, analytic expressions for the variance contributions, and the fidelity as a function of variations in the feedback gain.

[55] M. Pinard, P. F. Cohadon, T. Briant, and A. Heidmann, Phys. Rev. A **63,** 013808 (2000).

[56] C. Meng, G. A. Brawley, J. S. Bennett, M. R. Vanner, and W. P. Bowen, Phys. Rev. Lett. **125,** 043604 (2020).

[57] A. C. Doherty and K. Jacobs, Phys. Rev. A **60,** 2700 (1999).

[58] W. Bowen, N. Treps, B. Buchler, R. Schnabel, T. Ralph, T. Symul, and Ping Koy Lam, IEEE J. Sel. Top. Quantum Electron. **9,** 1519 (2003).

[59] S. Chountasis, L. K. Stergioulas, and A. Vourdas, J. Mod. Opt. **46,** 2131 (1999).

[60] D. J. Wilson, V. Sudhir, N. Piro, R. Schilling, A. Ghadimi, and T. J. Kippenberg, Nature (London) **524,** 325 (2015).